Available online at www.sciencedirect.com
SCIENCE DIRECT®
International Journal of Solids and Structures 42 (2005) 2243–2264
INTERNATIONAL JOURNAL OF SOLIDS and STRUCTURES
www.elsevier.com/locate/ijsolstr

Dynamic instability characteristics of laminated composite doubly curved panels subjected to partially distributed follower edge loading

L. Ravi Kumar [a,*], P.K. Datta [a,1], D.L. Prabhakara [b]

[a] Department of Aerospace Engineering, Indian Institute of Technology, Kharagpur 721 302, West Bengal, India
[b] Department of Civil Engineering, Malnad College of Engineering, Hassan 573 201, Karnataka, India

Received 30 April 2004; received in revised form 20 September 2004
Available online 2 November 2004

Abstract

This paper deals with the study of vibration and dynamic instability characteristics of laminated composite doubly curved panels, subjected to non-uniform follower load, using finite element approach. First order shear deformation theory is used to model the doubly curved panels, considering the effects of shear deformation and rotary inertia. The formulation is based on the extension of dynamic, shear deformable theory according to Sanders' first approximation for doubly curved laminated shells, which can be reduced to Love's and Donnell's theories by means of tracers. The modal transformation technique is applied to reduce the number of equilibrium equations for subsequent analysis. Structural damping is introduced into the system in terms of viscous damping. Instability behaviour of curved panels have been examined considering the various parameters such as width of edge load, load direction control, damping, influence of fiber orientation and lay up sequence etc. The results show that under follower loading the panel may lose its stability due to either flutter or divergence, depending on the system parameters.

Keywords: Follower force; Curved panels; Vibration; Dynamic stability

* Corresponding author. Tel.: +91 0806 601131; fax: +91 0806 614357.
E-mail addresses: ravibmsce@yahoo.com (L. Ravi Kumar), pkdatta@aero.iitkgp.ernet.in (P.K. Datta), cacep2001@yahoo.com (D.L. Prabhakara).
[1] Fax: +91 3222 255303.

0020-7683/$ - see front matter © 2004 Elsevier Ltd. All rights reserved.
doi:10.1016/j.ijsolstr.2004.09.024

Nomenclature

a, b	dimensions in the x and y directions respectively
c	load width parameter
E_{11}, E_{22}	Young's moduli of lamina along respective axes
P	resultant edge load
t	thickness
T	kinetic energy
U_1	strain energy associated with bending with transverse shear
U_2	work done by the initial in-plane stresses and the non-linear strain
$\{q\}$	nodal displacement vector
$[B]$	strain displacement matrix
$[C]$	damping matrix
$[D]$	flexural rigidity matrix
$[K]$	elastic stiffness matrix
$[K_G]$	stress stiffness matrix
$[K_{NC}]$	non-conservative matrix
$[M]$	mass matrix
$[\phi]$	modal matrix
v	Poisson's ratio
ρ	mass density
γ	non-dimensional load
λ	non-dimensional frequency
η	damping loss factor
φ	load direction control parameter
ω	angular frequency of transverse vibration
δW_{NC}	variational work done by non-conservative force

1. Introduction

Fiber-reinforced composite materials are extensively used in laminated thin-walled weight-sensitive structural parts of various modern engineering in the aerospace, mechanical, automotive and civil engineering sectors. In general, the forces acting on the structural elements can be classified into conservative and non-conservative forces. The follower force, the direction of which is configuration dependent, is a typical example of a non-conservative force. As the magnitude of the in-plane follower force acting over a thin panel is increased, the component may lose its stability at some stage. In dynamic analysis, the loss of stability can be identified by the way in which the natural frequencies alter with the increase of load. If any one of the eigenvalues reduces to zero with the increase of load, then the instability is by divergence (i.e. static instability). Many times it so happens that two natural frequencies coalesce with each other with the increase of load leading to the flutter type of instability. For example (i) the thrust exerted by the engines connected to the wing of an aircraft and (ii) highly flexible missiles, rockets and space vehicles changing orbit under end thrust are prone to either divergence or flutter types of instability.

Bolotin (1963) has studied non-conservative problems of elastic stability through classical approach. Initially, many researchers have focused their attention on the stability behaviour of one-dimensional elastic structures subjected to follower forces. Notable works in this field are of Herrmann and Jong (1965), Wu (1976), Ryu and Sugiyama (1994). Later, several research studies have concentrated on the stability of

two-dimensional structures, namely flat plates, subjected to follower forces. Culkowski and Reismann (1977) studied plate buckling due to follower edge forces using analytical method considering two boundaries. Farshad (1978) investigated the stability of cantilever plates subjected to biaxial subtangential load using Galerkin's method. Leipholz (1978) studied stability of a rectangular simply supported plate subjected to non-increasing tangential follower forces. Leipholz and Pfendt (1983) used Galerkin's theory to analyse the plate with distributed follower forces acting on the surface of the plate. Adali (1982) investigated stability behaviour of the plate subjected to a tangential follower force and an in-plane force for a clamped-free plate with two opposite simply supported edges. Higuchi and Dowell (1990, 1992) investigated the dynamic stability of completely free-edged rectangular flat plate by neglecting rotary inertia and shear deformation using modal analysis. It was observed that small damping has a predominant effect on the stability behaviour of a non-conservative system. Datta and Deolasi (1996) studied some aspects of dynamic instability characteristics of plates subjected to partially distributed follower edge loading with damping. Kim and Park (1998) investigated the dynamic stability behaviour of rectangular plates subjected to intermediate follower force. Choo and Kim (2000) studied the dynamic stability of isotropic and non-symmetric laminated rectangular plate with four free edges subjected to pulsating follower force. Kim and Kim (2000) studied dynamic stability of an isotropic, orthotropic and symmetrically laminated composite plate under pure follower force considering Mindlin assumption and investigated the effects of shear deformation and rotary inertia under follower force.

Bismarck-Nasr (1995) studied the stability behaviour of a cantilever cylindrically curved panel subjected to non-conservative tangential follower forces distributed over the surface and on the free end of the panel. Park and Kim (2000a,b, 2002) investigated, extensively, dynamic stability characteristics of a completely free cylindrical and stiff-edged cylindrical shell subjected to follower forces using finite element method.

Extensive review work have been reported by Qatu (1992), Liew et al. (1997) on shallow shell vibration and by Herrmann (1967), Komarakul-Na-Nakoran and Arora (1990), Bismarck-Nasr (1992), Langthjem and Sugiyama (2000) and Bazant (2000) on the systems subjected to non-conservative forces.

Most of the researchers have given importance to study the stability characteristics of plate/shell subjected to uniform edge follower forces. However, it is worth mentioning here that such loads are not very common in practice. Many practical situations demand the behavioural aspects of such structural elements under the action of discontinuous/partial edge follower forces with different non-conservative parameters. For example, the skin (panel) of the wing structure of an aircraft carries non-uniform partial in-plane load, making the panel susceptible to buckling. The resulting in-plane stress distribution in the panel, in general, is a combination of tensile and compression stress zones. In a certain domain, when the tensile zone dominates, it gives rise to a stiffening effect. On the other hand, domination of compressive zone leads to a destiffening behaviour. The results of such studies are not available in literature, which can be used in design practice. Further, dynamic stability analysis of composite panels subjected to follower forces is scanty and to the authors' knowledge, no such work is available in literature on the instability analysis of curved composite panels subjected to follower forces. Thus, there exists a wide scope to extend the research on composite curved panel type of structures. In the present work, the dynamic instability behaviour of laminated composite doubly curved panels (i.e. panels having certain prescribed curvature in x and y directions) subjected to non-uniform follower edge loading has been analysed, considering the effects of structural damping, load direction control and the lamination parameters.

2. Theory and formulations

The extended Hamilton principle is used to formulate the governing differential equilibrium equation for a doubly curved panel, taking in to account the work done by non-conservative forces.

The extended Hamilton principle (Kim and Kim, 2000) can be expressed as

$$\delta \int (T - U)\,\mathrm{d}t + \int \delta W_{\mathrm{NC}}\,\mathrm{d}t = 0 \tag{1}$$

The kinetic energy T of the curved panel can be expressed as

$$T = \frac{1}{2}\rho \int\int\int (\dot{u}^2 + \dot{v}^2 + \dot{w}^2)\,\mathrm{d}x\,\mathrm{d}y\,\mathrm{d}z \tag{2}$$

The strain energy U_1 associated with bending and transverse shear is given by

$$U_1 = \frac{1}{2}\int\int\left(\sum_{k=1}^{n}\int_{z_{k-1}}^{z_k}\{\varepsilon_l\}_k^{\mathrm{T}}[\overline{Q}]_k\{\varepsilon_l\}_k\,\mathrm{d}z\right)\mathrm{d}x\,\mathrm{d}y \tag{3}$$

where n is the number of layers, z_{k-1} and z_k are the distances from middle plane to the bottom and top of kth lamina. For the kth lamina with general ply orientation, the terms $\{\varepsilon_l\}_k$ and $[\overline{Q}]_k$ have been defined in Appendix A.

The expression for the non-linear strain energy due to the initial in-plane stresses and the non-linear strain is given by

$$U_2 = \frac{1}{2}\int\int\int\left[\{\sigma^0\}^{\mathrm{T}}\{\varepsilon_{\mathrm{nl}}\}\right]\mathrm{d}x\,\mathrm{d}y\,\mathrm{d}z \tag{4}$$

The expressions for the energies for a descretised panel can be written in matrix form as

$$U_1 = \frac{1}{2}\{q\}^{\mathrm{T}}[K]\{q\} \tag{5}$$

$$U_2 = \frac{1}{2}\{q\}^{\mathrm{T}}[K_{\mathrm{G}}]\{q\} \tag{6}$$

$$T = \frac{1}{2}\{\dot{q}\}^{\mathrm{T}}[M]\{\dot{q}\} \tag{7}$$

The matrices $[K]$, $[K_{\mathrm{G}}]$, $[M]$ and $\{q\}$ are the elastic flexural stiffness matrix, geometric stiffness matrix, consistent mass matrix and system displacement vector respectively. The system matrices have been derived using standard finite element procedure (Cook, 1987). Brief descriptions about the formulation of these are given in Appendix A.

δW_{NC} = Variation of the work done by the non-conservative forces, which consists of two parts: follower forces and damping forces

$$\delta W_{\mathrm{NC}} = \delta W_{\mathrm{F}} + \delta W_{\mathrm{D}} \tag{8}$$

where W_{D} and W_{F} are work done by the damping and follower forces respectively. $\delta W_{\mathrm{F}} = \sum_{i=1}^{l}\delta w_i(-P_i\theta_{y,i})$ where l is the number of nodes and P_i is the resultant in-plane follower force at ith node.

The variation of the work done by the normal component of the follower force $(-P_i\theta_{y,i})$, which is normal to the undeformed plane of the plate and acting opposite to the direction of w_i for $(0.0 < \varphi \leqslant 1.0)$ at the ith node is expressed as, $\delta W_{\mathrm{F},i} = \delta w_i(-P_i\theta_{y,i})$. This can be written in matrix form as

$$\delta W_{\mathrm{F},i} = \{\delta u_i, \delta v_i, \delta w_i, \delta\theta_{xi}, \delta\theta_{yi}\}^{\mathrm{T}}[0\quad 0\quad 1\quad 0\quad 0]^{\mathrm{T}}[-P_i][0\quad 0\quad 0\quad 0\quad 1]\{u_i, v_i, w_i, \theta_{xi}, \theta_{yi}\}$$

or in abbreviated form

$$\delta W_{\mathrm{F},i} = \{\delta q\}_i^{\mathrm{T}}[N]_i^{\mathrm{T}}[-P]_i[N_{\mathrm{d}}]_i\{q\}_i$$

Considering the components of the forces at all the nodes, the variation of work can be written in matrix form as

$$\delta W_{\mathrm{F}} = \{\delta q\}^{\mathrm{T}}[N]^{\mathrm{T}}[P][N_{\mathrm{d}}]\{q\}$$

in which $\{q\}$ is the overall displacement vector,

$$[N] = [[N]_1[N]_2[N]_3 \cdots [N]_i \cdots [N]_l]$$

and

$$[P] = -\mathrm{diag}[[P]_1[P]_2[P]_3 \cdots [P]_i \cdots [P]_l]$$

The variation of the work done by the non-conservative forces can be written in the following form:

$$\delta W_{\mathrm{F}} = \{\delta q\}^{\mathrm{T}}[K_{\mathrm{NC}}]\{q\} \tag{9}$$

in which $[K_{\mathrm{NC}}] = [N]^{\mathrm{T}}[P][N_{\mathrm{d}}]$ is the unsymmetric follower force matrix.

The variation of the work done by the damping forces can be written in matrix form as

$$\delta W_{\mathrm{D}} = \{\delta q\}^{\mathrm{T}}[C]\{\dot{q}\} \tag{10}$$

Substituting the energy expressions in Eq. (1) and upon simplification, the following equilibrium equation for the panel is obtained:

$$[M]\{\ddot{q}\} + [C]\{\dot{q}\} + [K]\{q\} - P[[K_{\mathrm{G}}] + [K_{\mathrm{NC}}]]\{q\} = 0 \tag{11}$$

$$[M]\{\ddot{q}\} + [C]\{\dot{q}\} + [K]_{\mathrm{eff}}\{q\} = \{0\} \tag{12}$$

where $[K]_{\mathrm{eff}} = [K] - P[[K_{\mathrm{G}}] + [K_{\mathrm{NC}}]]$.

In Eq. (12) $\{q\}$ is the nodal displacement vector and P is the magnitude of the applied load. The matrix $[K_{\mathrm{G}}]$ takes into account all the in-plane forces, including the in-plane (conservative) component of the applied load, while the matrix $[K_{\mathrm{NC}}]$ takes into account the non-conservative component of the follower load that is in a direction perpendicular to the undeformed mid-plane of the panel. All the relevant matrices are given in Appendix A. At the end, as $[K_{\mathrm{NC}}]$ is non-symmetric, the effective stiffness matrix $[K_{\mathrm{eff}}]$ will also be non-symmetric and hence the equilibrium Eq. (12) leads to a non-self-adjoint eigenvalue problem for non-zero P.

For sinusoidal motion of the panel, structural damping matrix can be expressed in terms of an equivalent viscous damping matrix as follows:

$$[C] = \frac{\eta}{\omega}[K] \tag{13}$$

where η is the loss factor for the panel material and ω is the frequency of flexural vibration of the panel.

2.1. Modal transformation

The sizes of the various matrices in Eq. (11) are very large and equal to the number of active degrees of freedom (say n). The solution of this equation in its original form may be prohibitive, particularly for determining the flutter load. Hence, a modal transformation is applied to Eq. (11) to reduce its size and to retain only the most dominant modes of vibration corresponding to the first few eigenvalues starting from the lowest frequency of vibration.

The equilibrium equation for the free vibration of an undamped unloaded panel can be written as

$$-\omega^2[M]\{q_0\} + [K]\{q_0\} = 0 \tag{14}$$

where ω is the angular natural frequency of free vibration and $\{q_0\}$ is the corresponding modal vector. Here, subspace iteration method is used to extract only first few eigenvalues and corresponding eigenvectors (say m). Then the modal matrix $[\phi]$ will have m number of modal vectors with each vector consisting of n number of elements. Hence the size of the modal matrix will be $m \times n$.

Let the displacement vector be expressed as

$$\{q\} = [\phi]\{\xi\} \tag{15}$$

where $\{\xi\}$ are normal co-ordinates of size $m \times 1$.

Substituting Eq. (15) in Eq. (11) and premultiplying by $[\phi]^{\mathrm{T}}$, the following m number of equilibrium equations are obtained:

$$[\phi]^{\mathrm{T}}[M][\phi]\{\ddot{\xi}\} + [\phi]^{\mathrm{T}}[C][\phi]\{\dot{\xi}\} + [\phi]^{\mathrm{T}}[K][\phi]\{\xi\} - P[\phi]^{\mathrm{T}}[[K_{\mathrm{G}}] + [K_{\mathrm{NC}}]][\phi]\{\xi\} = \{0\}$$

After triple multiplication, the above equation reduces to

$$\{\ddot{\xi}\} + [\widehat{C}]\{\dot{\xi}\} + [[\Lambda] - P[\widehat{K}_{\mathrm{G}}]]\{\xi\} = 0 \tag{16}$$

where $[\widehat{C}] = [\phi]^{\mathrm{T}}[C][\phi]$ and $[\widehat{K}_{\mathrm{G}}] = [\phi]^{\mathrm{T}}[[K_{\mathrm{G}}] + [K_{\mathrm{NC}}]][\phi]$; $[\Lambda]$ is a diagonal matrix containing the eigenvalues of Eq. (14), that is squares of the natural frequencies of free vibration of the unloaded panel.

Using Eq. (13) $[\widehat{C}]$ can be expressed as

$$[\widehat{C}] = \frac{\eta}{\omega}[\Lambda] \tag{17}$$

Now considering the motion of the panel in the form $\{\xi\} = \{\xi_0\}\mathrm{e}^{\mathrm{i}\omega t}$, Eq. (16) changes to

$$\begin{aligned} &-\omega^2\{\xi_0\} + \mathrm{i}\eta[\Lambda]\{\xi_0\} + ([\Lambda] - P[\widehat{K}_{\mathrm{G}}])\{\xi_0\} = 0 \quad \text{or} \\ &-\omega^2\{\xi_0\} + [(1+\mathrm{i}\eta)[\Lambda] - P[\widehat{K}_{\mathrm{G}}]]\{\xi_0\} = 0 \end{aligned} \tag{18}$$

Eq. (18) is an eigenvalue problem with eigenvalues ω^2, which are the squares of the natural frequencies of vibration under follower load P. Eq. (18) can be solved by using standard eigenvalue routine for a complex general matrix. The imaginary part of ω corresponds to the exponential increment or decrement of the amplitude of vibration. The system is unstable when any of the values of ω of Eq. (18) has a negative imaginary part. Further, during the transition from stability to instability if the real part of ω is zero, then the instability occurs due to divergence. Otherwise instability occurs due to flutter.

3. Problem definition

The basic configuration of the problem considered here is a laminated composite doubly curved panel (Librescu et al., 1989; Qatu and Leissa, 1991; Liew et al., 1997) as shown in Fig. 1. Fig. 2 shows the plan view of the curved square panel subjected to partial follower edge load of width 'c' at the free edge at $x = a$ (free edge) such that the load always maintains a direction that is perpendicular to the normal of the loaded edge. In the present analysis, two boundary conditions C–F–F–F ($x = 0$ and a; clamped and free, $y = 0$ and b; free and free) and C–F–S–S ($x = 0$ and a; clamped and free, $y = 0$ and b; simply supported) have been chosen. Here C–F–F–F refers to a typical cantilever panel, which is very sensitive to the follower load compared to panels with other boundary conditions. However, in order to study the effect of edge restraints by retaining the symmetry with respect to x-axis the edges parallel to this axis have been restrained by providing simple supports (C–F–S–S). An eight nodded curved isoparametric quadratic element is used in the present analysis with five degrees of freedom u, v, w, θ_x and θ_y per node. First order shear deformation theory (FSDT) is used and the shear correction factor of $\frac{5}{6}$ (Librescu et al., 1989; Chandrashekhara, 1989) has been employed to account for the non-linear distribution of shear strain through the thickness. See Appendix B

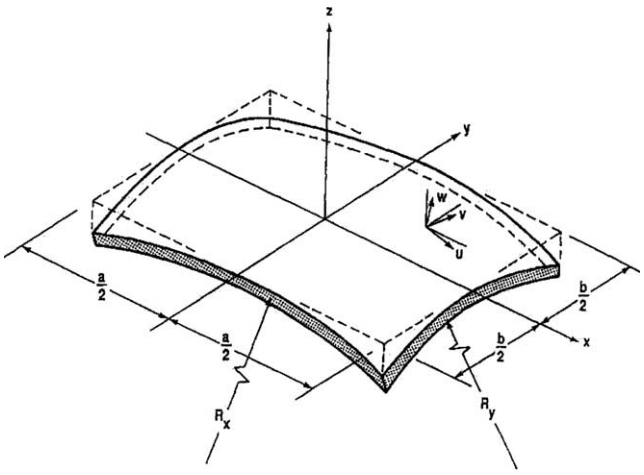

Fig. 1. Geometry and co-ordinate system of a laminated composite doubly curved panel.

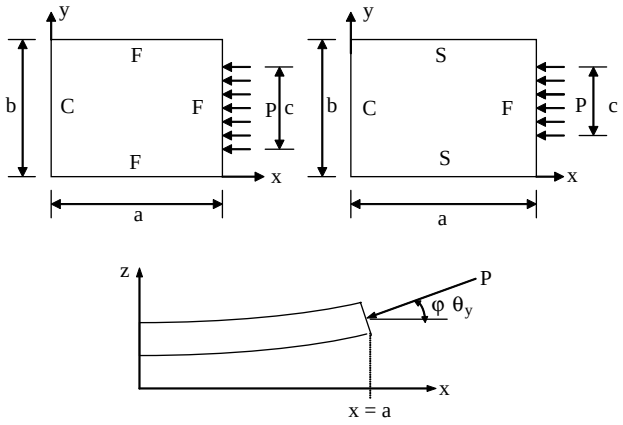

Fig. 2. Curved panels under partial follower edge loading.

for the details. The constitutive relationships (Sahu and Datta, 2001; Chandrashekhara, 1989) and kinematic relations (Chandrashekhara, 1989; Reddy, 1984) for doubly curved panels are used. In the present problem cross-ply and angle-ply laminated curved panels having a/R_x and b/R_y ratios of $(0.0, 0.0)$ $(0.2, 0.2)$ $(0.0, 0.2)$ and $(-0.2, 0.2)$ for flat, spherical, cylindrical and hyperbolic paraboloidal panels respectively are considered. The ratio of length to breadth (a/b) is 0.5, 1; ratio of breadth to thickness (b/t) is 100 and load width parameter (c/b) ranges from 0.2 to 1. The material characteristic parameters of $E_{11}/E_{22} = 40$, $G_{12} = G_{13} = 0.6E_{22}$, $G_{23} = 0.5E_{22}$ and $v = 0.25$ were considered. Unless otherwise stated the boundary conditions employed in the present analysis are

(a) On edges parallel to y-axis (i) simply supported, S: $v = w = \theta_y = 0$; (ii) clamped, C: $u = v = w = \theta_x = \theta_y = 0$ and (iii) free, F: no restraints.
(b) On edges parallel to x-axis (i) simply supported, S: $u = w = \theta_x = 0$; (ii) clamped, C: $u = v = w = \theta_x = \theta_y = 0$ and (iii) free, F: no restraints.

In the present analysis, non-dimensional frequencies and buckling loads are represented by the following definitions:

$$\lambda = \omega b^2 \sqrt{(\rho/E_{22}t^2)} \quad \text{and}$$

$$\gamma = Pa^2/E_{22}bt^3$$

where P is the resultant edge load and the other relevant symbols have been explained in the 'Notation'.

4. Results and discussion

Convergence and comparison studies have been carried out for fundamental frequencies of vibration of cantilevered laminated doubly curved panels (flat, spherical, cylindrical, hyperbolic paraboloidal) and the results are compared with those of Qatu and Leissa (1991) in Table 1.

Based on the above convergence study, a 10×10 mesh has been employed to discretize the panel in the subsequent analysis. Table 2 shows the non-dimensional buckling loads for cylindrical panels with different breadth to thickness ratios and the same are compared with those of Sciuva and Carrera (1990). To validate the present model subjected to non-conservative (follower) load, the results are compared with Adali (1982)

Table 1
Convergence of non-dimensional fundamental frequencies without in-plane load of cantilevered doubly-curved panels $a/b = 1$, $b/t = 100$, $b/R_y = 0.1$, $E_{11} = 138\,\text{GPa}$, $E_{22} = 8.96\,\text{GPa}$, $G_{12} = 7.1\,\text{GPa}$, $v = 0.3$, non-dimensional frequency, $\lambda = \omega b^2\sqrt{(\rho/E_{11}t^2)}$

Mesh division	Non-dimensional frequencies of shells			
	Plate	Cylindrical	Spherical	Hyp-paraboloid
0/90/0				
4×4	0.9995	1.2477	1.1746	1.1508
8×8	0.9993	1.2473	1.1715	1.1477
10×10	0.9998	1.2473	1.1715	1.1476
	0.9998[a]	1.2479[a]	1.1721[a]	1.1478[a]
45/−45/45				
4×4	0.4615	0.7277	0.6945	0.6585
8×8	0.4596	0.7210	0.6839	0.6465
10×10	0.4592	0.7197	0.6825	0.6452
	0.4607[a]	0.7197[a]	0.6845[a]	0.6448[a]

[a] Qatu and Leissa (1991).

Table 2
Comparison of non-dimensional compressive buckling loads, for square simply supported symmetric cross-ply (0/90/0/90/0), cylindrical shell panel ($a/b = 1$, $R/a = 20.0$, $E_{11} = 40E_{22}$, $G_{12} = G_{13} = 0.5E_{22}$, $G_{23} = 0.6E_{22}$, $v_{12} = v_{13} = 0.25$)

	Buckling load for different b/t			
b/t	10	20	50	100
Present	23.9655	31.7944	35.3974	36.8474
FSDT[a]	24.19	31.91	35.42	36.86
CST[a]	35.84	35.88	36.13	37.04

[a] Sciuva and Carrera (1990).

Table 3
Comparison of non-dimensional flutter loads γ_{cr} and non-dimensional flutter frequencies λ_{cr} for an isotropic C–F–S–S plate $c/b = 1.0$ and $v = 0.3$

Aspect ratio	Flutter load γ_{cr}			Flutter frequency λ_{cr}		
a/b	Present	Adali (1982)	Datta and Deolasi (1996)	Present	Adali (1982)	Deolasi (1996)
1.0	51.651	51.650	52.06	16.685	16.67	16.33
0.5	26.923	27.11	27.20	49.567	49.58	49.30

and Deolasi (1996) in Table 3 and the numerical results of critical flutter load and flutter frequencies are found to be in good agreement.

4.1. Follower edge load on cross-ply laminated panels

Figs. 3–5 show the variation of the real part of the natural frequency Re(λ) with applied follower load γ, for spherical, cylindrical and hyperbolic paraboloidal panels respectively for the first flutter mode. In this analysis, 0/90/0 and 0/90/90/0 cross-ply laminated cantilever panels are considered with ratios $a/b = 1$, $b/t = 100$ and $c/b = 1$. In this case, the end follower load is uniformly distributed at the edge opposite to the fixed edge. From the figure, it is observed that at a certain value of the load, the two frequencies coalesce and beyond this value of load, the two frequencies become complex conjugate with one having negative imaginary part. This is the condition, which corresponds to flutter. The load and frequency at which coalesce of frequencies occurs are termed as the flutter load γ_{cr} and flutter frequency λ_{cr} respectively.

From the figures, it is observed that for the given geometry, boundary conditions and load parameter, the flutter load is less affected by ply layups for the spherical panel. However, for the cases of cylindrical and hyperbolic paraboloidal panels, 0/90/0 ply layup showed higher flutter load. This may be due to the higher stiffness of these two panels for the given ply layup.

Table 4 shows the numerical results of flutter load and frequency for 0/90, 0/90/0, 0/90/90/0 layups for each of spherical, cylindrical and hyperbolic paraboloidal panels having aspect ratio $a/b = 1$, breadth to thickness ratio $b/t = 100$, subjected to end follower load at the free edge having load width ratios (c/b) of 0.2, 0.4, 0.6, 0.8 and 1. It is noticed from the table that the magnitude of the flutter load and frequencies

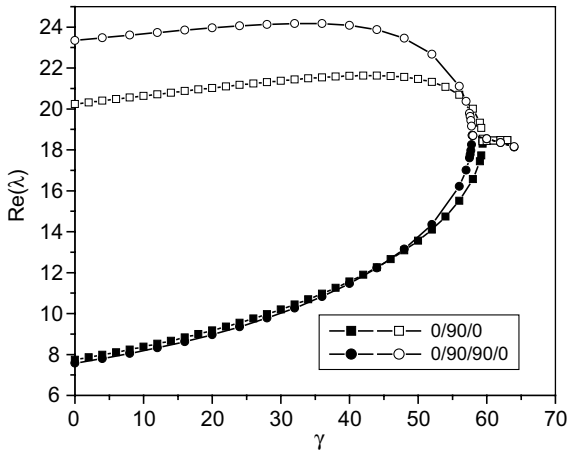

Fig. 3. Non-dimensional natural frequency Re(λ) versus non-dimensional follower force γ for C–F–F–F spherical panel.

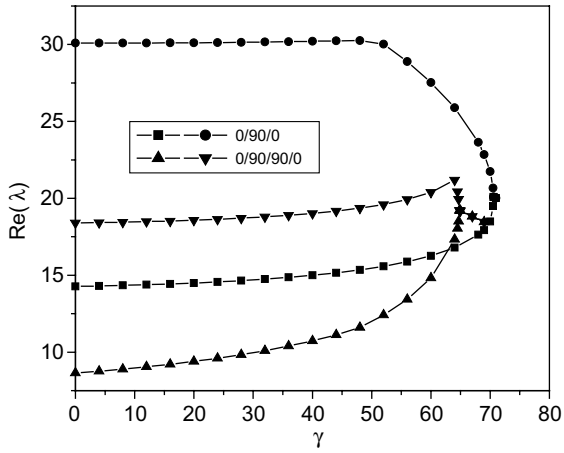

Fig. 4. As Fig. 3, but cylindrical panel.

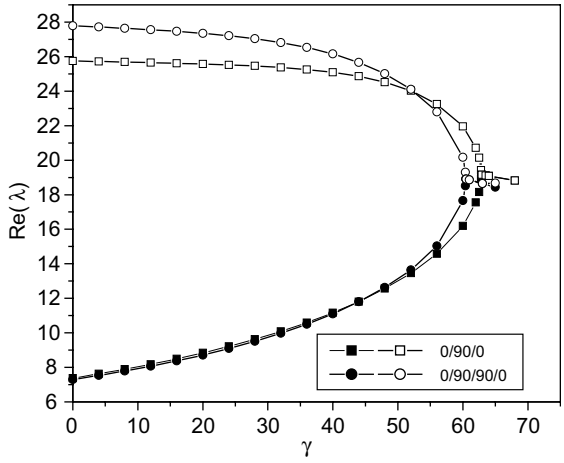

Fig. 5. As Fig. 3, but hyperbolic paraboloidal panel.

are changing appreciably with load width ratio (c/b). It may be concluded from the table that for certain panel geometry, critical buckling load, γ_{cr} usually decreases as c/b increases (CFFF boundary). However, for c/b transition from 0.8 to 1, γ_{cr} increases again. This can be attributed to the fact that as the load width approaches the full edge, boundary restraint causes higher buckling load.

Table 5 shows critical flutter load (γ_{cr}) for $a/b = 0.5$, $b/t = 100$ for 0/90/0 and 0/90/90/0 C–F–S–S laminated panels. From the table it is observed that the critical flutter load is changing appreciably with the load width ratio and the aspect ratio.

The effect of ply layups on flutter loads of the panels for the given geometry, boundary conditions and load parameter is further illustrated in Figs. 6 and 7. Three ply layups 0/90, 0/90/0, 0/90/90/0 have been considered. From the figures, it is observed that the number of layers and ply orientations have very significant effect on the dynamic stability characteristics for different layups. The variations in the

Table 4
Non-dimensional critical flutter load and frequencies for laminated cross-ply curved panels for $a/b = 1$, $b/t = 100$ with different ply orientations and load width ratios

c/b ratio	0/90		0/90/0		0/90/90/0	
	γ_{cr}	λ_{cr}	γ_{cr}	λ_{cr}	γ_{cr}	λ_{cr}
Spherical panel						
C–F–F–F condition						
0.2	21.98	10.5648	42.68	31.1812	38.72	31.2395
0.4	21.04	10.5057	50.92	29.2040	46.08	29.6540
0.6	19.02	10.4117	65.56	25.9260	59.58	26.7233
0.8	16.48	10.2959	57.94	16.8124	60.68	17.9470
1.0	14.38	10.2731	59.42	18.4189	57.88	18.7071
C–F–S–S condition						
0.2	24.94	38.4344	18.26	50.2713	49.18	75.7609
0.4	29.56	37.045	27.46	48.783	67.36	31.8624
0.6	36.34	35.7183	42.18	47.4435	78.26	30.9957
0.8	41.02	40.9270	97.92	30.0668	92.32	45.6664
1.0	47.54	40.4200	113.20	41.4227	105.50	45.6987
Cylindrical panel						
C–F–F–F condition						
0.2	12.64	19.4779	39.84	26.1496	37.30	27.3124
0.4	13.70	19.1703	46.20	25.0577	42.98	26.3055
0.6	15.24	18.6917	42.50	32.9229	52.90	25.0795
0.8	17.26	17.9412	43.40	31.9895	66.18	23.6503
1.0	12.88	18.3442	70.58	20.0802	64.82	19.2167
C–F–S–S condition						
0.2	23.8	14.3968	10.66	42.6567	49.08	25.1130
0.4	26.42	14.0974	14.86	42.084	53.7	24.2472
0.6	24.18	31.3254	22.08	41.4484	61.48	34.7552
0.8	24.72	31.3308	29.72	41.2705	62.8	34.9031
1.0	31.52	30.6515	86.04	27.6056	80.18	34.1986
Hyperbolic paraboloidal panel						
C–F–F–F condition						
0.2	14.22	11.795	25.12	30.8181	23.86	31.2907
0.4	14.44	11.2952	29.94	29.8788	28.10	30.5076
0.6	15.16	10.9668	37.70	38.3431	36.42	29.3078
0.8	16.18	10.7535	55.50	26.7002	56.00	26.4095
1.0	16.88	8.9762	62.84	19.1567	60.46	18.9108
C–F–S–S condition						
0.2	4.74	21.3327	30.62	28.717	28.68	28.1613
0.4	5.20	21.3122	33.92	28.0666	31.74	27.8309
0.6	6.00	21.2775	39.92	27.6320	36.98	27.5470
0.8	7.14	21.2444	48.48	27.3824	44.52	27.3025
1.0	8.66	21.2050	59.82	27.1756	54.90	27.0707

flutter frequency and load can be attributed to the fact that the ply layups significantly alter the stiffness characteristics of the panels for the given geometry, boundary conditions and the load parameter. It is also observed that the variation of the real part of natural frequency $\mathrm{Re}(\lambda)$ is significantly affected by the applied follower load for spherical, cylindrical and hyperbolic paraboloidal panels for the flutter mode.

Table 5
Non-dimensional critical flutter load for C–F–S–S laminated cross-ply curved panels with $a/b = 0.5$, $b/t = 100$ with different load width ratios

c/b ratio	Spherical		Cylindrical		Hyper-paraboloidal	
	0/90/0	0/90/90/0	0/90/0	0/90/90/0	0/90/0	0/90/90/0
C–F–F–F condition						
0.2	17.315	14.035	17.505	14.265	15.115	11.310
0.4	26.605	21.520	26.450	21.625	23.430	17.425
0.6	39.300	18.595	38.755	31.970	34.745	26.200
0.8	17.585	24.395	51.540	47.480	45.390	34.425
1.0	34.920	37.330	61.425	56.385	51.525	48.520
C–F–S–S condition						
0.2	9.505	17.485	10.585	17.210	7.000	15.145
0.4	17.005	22.480	18.730	21.840	12.560	16.605
0.6	23.340	25.810	27.760	24.970	22.715	18.705
0.8	31.135	33.890	36.915	33.065	32.850	24.780
1.0	67.130	62.025	64.820	59.865	59.430	54.290

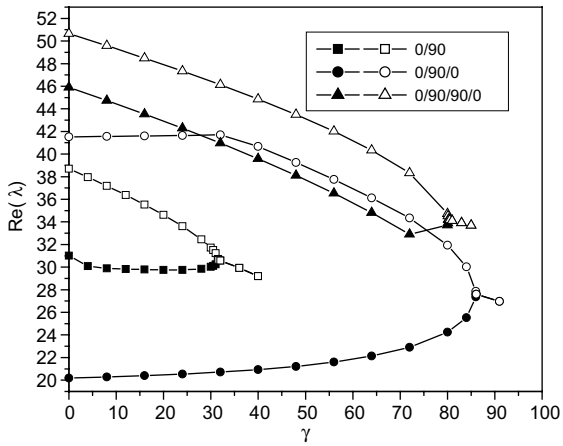

Fig. 6. Non-dimensional natural frequency Re(λ) versus non-dimensional follower load γ for C–F–S–S cross-ply laminated cylindrical panel for $a/b = 1$, $c/b = 1$, $b/t = 100$ for the first flutter mode.

4.2. Follower edge load on angle-ply laminated panels

Figs. 8 and 9 show the variation of frequency with the load for the first flutter mode for C–F–S–S spherical and cylindrical panels having ply orientation of $\theta/-\theta/\theta$, θ having values of 15, 30, 45, 60, 75 degrees respectively. In this example, the follower force is acting at the free edge of the panel. From the figures it is observed that the value of the critical load substantially changes with ply angle of the laminate. Table 6 shows numerical results for cantilevered C–F–F–F panels having three different ply orientations 45/−45, 45/−45/45 and 45/−45/45/−45 with $a/b = 1$ and $b/t = 100$. From the table it is observed that the critical load is significantly affected by load width ratio (c/b) for all ply orientations. Maximum critical load occurs at $c/b = 0.2$ for the spherical panel. However, for cylindrical and hyperbolic paraboloidal panels, critical load increases with load width.

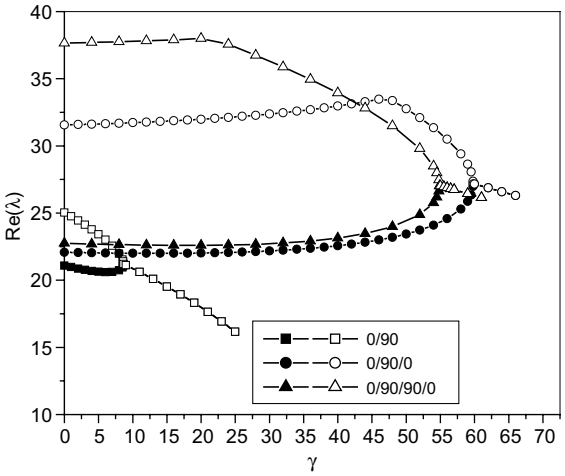

Fig. 7. As Fig. 6, but for hyperbolic paraboloidal panel.

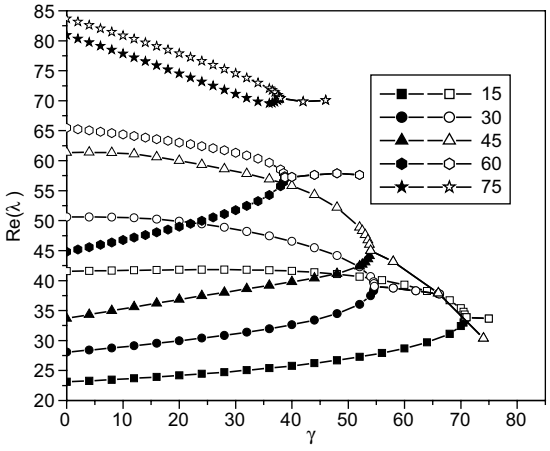

Fig. 8. Non-dimensional natural frequency Re(λ) versus non-dimensional follower load γ for C–F–S–S angle-ply $\theta/-\theta/\theta$ laminated spherical panel for $a/b = 1$, $c/b = 1$, $b/t = 100$ for the first flutter mode.

4.3. Effects of damping parameter

In the presence of damping, eigenfrequencies of the panels are always complex quantities irrespective of the panel is stable or not. However, before the loss of stability by flutter the imaginary parts of the eigenvalues are always positive. Fig. 10(a) and (b) show the real and imaginary part of the complex frequency λ for 0/90/0 laminated hyperbolic paraboloidal panel for $a/b = 1$, $b/t = 100$ and $c/b = 1$ with three damping levels, $\eta = 0.0$, 0.02 and 0.1. From the analysis it is observed that when $\eta = 0$, the two real frequencies merge together into a pair of conjugate complex frequency ($\lambda = \mathrm{Re}(\lambda) \pm \mathrm{Im}(\lambda)$) at γ_{cr} (59.82) (Fig. 10) to form a flutter mode. As γ is increased beyond γ_{cr}, there is a rapid increase in the imaginary parts of the natural frequencies. Since one of the frequencies has a negative imaginary part, the panels undergo strong flutter.

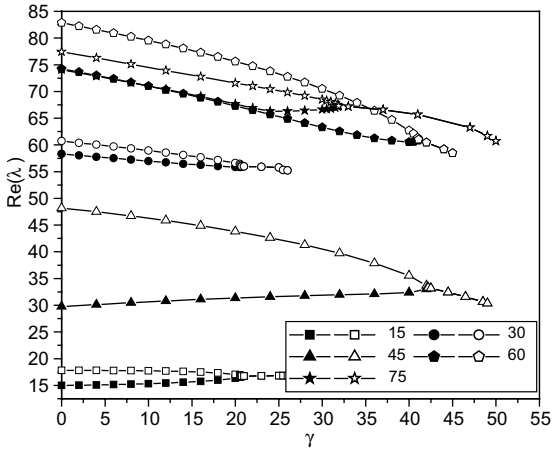

Fig. 9. As Fig. 8, but for cylindrical panel.

Table 6
Non-dimensional critical flutter loads for laminated C–F–F–F angle-ply curved panels with different ply orientations and different of load width ratios

Type of panel	Ply-orientation	c/b ratio				
		0.2	0.4	0.6	0.8	1.0
		Non-dimensional critical load γ_{cr}				
Spherical	45/−45	9.86	9.76	9.62	9.46	9.44
	45/−45/45	11.94	11.58	11.18	10.84	9.38
	45/−45/45/−45	16.48	16.34	16.14	16.00	16.08
Cylindrical	45/−45	7.42	8.06	8.98	10.02	11.18
	45/−45/45	8.38	9.22	11.08	15.30	15.72
	45/−45/45/−45	20.02	20.82	21.60	22.26	23.02
Hyperbolic paraboloid	45/−45	7.98	8.52	9.28	10.22	16.82
	45/−45/45	5.90	6.32	6.82	7.42	8.04
	45/−45/45/−45	21.94	22.76	23.46	24.00	28.54

If $\eta \neq 0$, the two curves corresponding to the real part of the frequencies do not merge, but approach each other (Fig. 10(a)) and initially both eigencurves have positive imaginary parts (Fig. 10(b)). However, as γ is increased, the imaginary part of the first frequency gradually changes from positive to negative (crosses zero frequency line) at γ^*_{cr} at 54.56 and 56.18 for $\eta = 0.02$ and 0.1 respectively. This means that the flutter in the presence of damping occurs at a lower load as compared to that without damping. The negative imaginary part of the first natural frequency implies that there is a negative effective damping in the first mode for γ greater than γ^*_{cr}.

Table 7 shows the numerical results for the critical flutter load for spherical, cylindrical and hyperbolic paraboloidal panels with different c/b ratios and damping factors. In the results presented, 0/90, 0/90/0, 0/90/90/0 cross-ply laminated panels with three different damping levels $\eta = 0$, 0.02 and 0.1 are considered. In general, it is noticed from the table that the damping has a significant effect on the flutter behaviour (stabilizing or destabilizing) of the laminated panels with the type of ply and the angle of orientations subjected to follower loading.

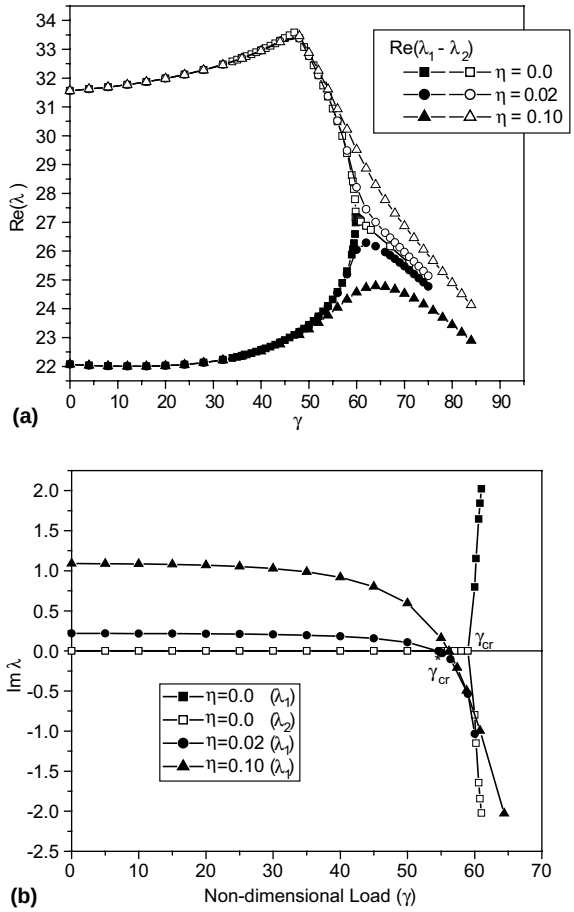

Fig. 10. (a) Non-dimensional natural frequency (Real part (λ)) versus non-dimensional follower load γ for C–F–S–S 0/90/0 laminated hyperbolic paraboloidal panel for $a/b = 1$, $c/b = 1$, $b/t = 100$ for the first flutter mode with damping factors. (b) As Fig. 10(a), but for imaginary part of the frequency.

4.4. Effect of load direction control parameter

The follower force considered in the previous sections was a tangential force with the value of $\varphi = 1$. However, it is possible to consider a follower force that maintains an angle $\varphi\theta_y$ at the edge, where φ is a direction control parameter as shown in Fig. 2. The loading in this case is called the controlled follower force. Such a force can be realized by means of some direction control mechanism. In this case, the free vibration, divergence and flutter problems can be solved by simply replacing the matrix $[K_{NC}]$ by $\varphi[K_{NC}]$ in Eq. (11). The value of φ ranges from 0 to 1. For $\varphi = 0$, the system is conservative and only divergence instabilities exist.

Fig. 11 shows the effect of different φ on the real part of the natural frequency with different c/b ratios for a C–F–S–S hyperbolic paraboloidal panel having 0/90/0 ply orientation subjected to uniformly distributed follower edge load at the free edge. It is observed that the increase in the direction control parameter of the follower load has a stabilizing behaviour. Similar results were observed for the case of spherical panel. This behaviour is similar to that of an isotropic flat panel (Deolasi, 1996). However, in the case of cylindrical panel, increasing direction control parameter gives a destabilizing effect for the narrow partial follower edge load.

Table 7
Non-dimensional critical flutter load for laminated cross-ply C–F–S–S laminated curved panels with effect of damping, different ply orientations and positions of load width ratio

Type of panel	Layup	Damping parameter	c/b ratio				
			0.2	0.4	0.6	0.8	1.0
			Non-dimensional critical load γ_{cr}				
Spherical	0/90	0.0	24.94	29.56	36.34	41.02	47.54
		0.02	18.70	21.42	25.72	31.44	38.50
		0.1	18.84	21.60	25.94	31.72	32.84
	0/90/0	0.0	18.26	27.46	42.18	97.92	113.2
		0.02	18.42	27.86	44.62	55.56	71.56
		0.1	25.06	37.56	44.96	56.10	72.18
	0/90/90/0	0.0	49.18	67.36	78.26	92.32	105.5
		0.02	34.14	38.58	46.28	57.40	74.72
		0.1	34.38	38.88	46.66	57.90	74.72
Cylindrical	0/90	0.0	23.80	26.42	24.18	24.72	31.52
		0.02	20.78	23.12	23.84	23.90	22.72
		0.1	21.30	23.68	27.62	27.78	32.26
	0/90/0	0.0	10.66	14.86	22.08	29.72	86.04
		0.02	10.90	15.28	23.38	57.66	75.18
		0.1	17.32	38.18	46.58	58.32	76.16
	0/90/90/0	0.0	49.08	53.70	61.48	62.80	80.18
		0.02	34.28	38.64	46.12	57.04	74.68
		0.1	34.64	39.08	46.68	57.76	75.78
Hyperbolic paraboloid	0/90	0.0	4.74	5.20	6.00	7.14	8.66
		0.02	4.74	5.22	6.02	7.20	8.78
		0.1	5.88	6.50	7.54	9.06	11.06
	0/90/0	0.0	30.62	33.92	39.92	48.48	59.82
		0.02	27.06	30.38	36.04	43.96	54.56
		0.1	27.68	31.14	37.02	45.18	56.18
	0/90/90/0	0.0	28.68	31.74	36.98	44.52	54.90
		0.02	26.00	28.94	33.88	40.92	50.76
		0.1	26.70	29.78	34.90	42.22	52.50

5. Conclusions

The results from the dynamic instability analysis of the laminated composite panels subjected to partially distributed follower edge loading can be summarized as follows:

Follower loading on the free edges may imply flutter type of instability beyond a certain value of the follower load due to coalescence of two frequencies into a complex conjugate pair. Flutter is observed to be more common than divergence under follower loading.

The critical flutter condition generally decreases (more susceptible to flutter) with increasing load width upto a particular value and then it increases as the load width extends over the entire edge of the plate/panel.

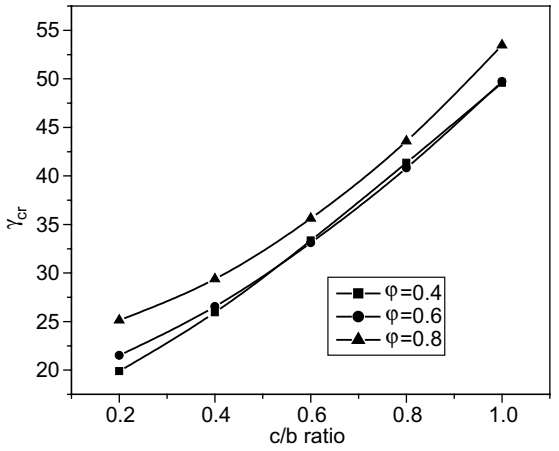

Fig. 11. Effect of load direction control parameter on non-dimensional critical flutter load γ_{cr} with load width ratio c/b for C–F–S–S cross-ply 0/90/0 laminated hyperbolic paraboloidal panel having $a/b = 1$, $c/b = 1$, $b/t = 100$ for the first flutter mode.

Damping in the system is found to have a significant effect on the flutter behaviour of curved panel, depending on the ply orientations of different panel geometries and load width ratios. In most cases, the damping effect gives destabilizing behaviour making the panel prone to flutter. The destabilizing effect of damping implies that the effective damping becomes negative beyond a certain load in one of the two modes as the imaginary part of the eigenvalue becomes negative giving rise to the flutter phenomenon. However, it is difficult to explain the above phenomenon, both, physically and mathematically.

Type of ply orientation, number of lay-ups and ply angle affect significantly the stability behaviour under distributed and partially distributed follower edge load.

Direction control parameter significantly affects the critical flutter load, showing both the effects of stabilizing and destabilizing behaviour depending on the panel geometry. In the cases of spherical and hyperbolic paraboloidal panels, the effect is stabilizing and for the case of cylindrical panel, it shows destabilizing behaviour.

Appendix A

The reduced stress–stain relations for an orthotropic kth layer under a plane stress assumption ($\sigma_z = 0$) with reference to the principal directions of the lamina is

$$\begin{Bmatrix} \sigma_1 \\ \sigma_2 \\ \tau_{12} \\ \tau_{23} \\ \tau_{31} \end{Bmatrix}_k = \begin{bmatrix} Q_{11} & Q_{12} & & & \\ Q_{12} & Q_{22} & & & \\ & & Q_{66} & & \\ & & & Q_{44} & \\ & & & & Q_{55} \end{bmatrix}_k \begin{Bmatrix} \varepsilon_1 \\ \varepsilon_2 \\ \gamma_{12} \\ \gamma_{23} \\ \gamma_{31} \end{Bmatrix}_k \tag{A.1}$$

Premultiplying the above by the transpose of a suitable rotation matrix i.e. $[R]^T$ and then postmultiplying by $[R]$, we can arrive at the stiffness matrix $[\overline{Q}]$ of a lamina with reference to the x–y axes as given below:

$$\begin{Bmatrix} \sigma_x \\ \sigma_y \\ \tau_{xy} \\ \tau_{yz} \\ \tau_{zx} \end{Bmatrix}_k = \begin{bmatrix} \overline{Q}_{11} & \overline{Q}_{12} & \overline{Q}_{16} & & \\ \overline{Q}_{12} & \overline{Q}_{22} & \overline{Q}_{26} & & \\ \overline{Q}_{16} & \overline{Q}_{26} & \overline{Q}_{66} & & \\ & & & \overline{Q}_{44} & \overline{Q}_{45} \\ & & & \overline{Q}_{45} & \overline{Q}_{55} \end{bmatrix}_k \begin{Bmatrix} \varepsilon_x \\ \varepsilon_y \\ \gamma_{xy} \\ \gamma_{yz} \\ \gamma_{zx} \end{Bmatrix}_k \tag{A.2}$$

Using the classical lamination theory, the linear strain in any lamina can be expressed in terms of middle plane strains and curvatures as

$$\begin{Bmatrix} \varepsilon_x \\ \varepsilon_y \\ \gamma_{xy} \\ \gamma_{yz} \\ \gamma_{zx} \end{Bmatrix}_l = \begin{Bmatrix} \varepsilon_x^0 \\ \varepsilon_y^0 \\ \gamma_{xy}^0 \\ \gamma_{yz}^0 \\ \gamma_{zx}^0 \end{Bmatrix} + z \begin{Bmatrix} \kappa_x \\ \kappa_y \\ \kappa_{xy} \\ \kappa_{yz} \\ \kappa_{zx} \end{Bmatrix} \tag{A.3}$$

Using the constitutive relation given in Eq. (A.2), one can establish the relation between the stress resultants with that of the middle plane strains and curvatures for the laminate as given below:

$$\begin{Bmatrix} N_i \\ M_i \\ Q_i \end{Bmatrix} = \begin{bmatrix} A_{ij} & B_{ij} & 0 \\ B_{ij} & D_{ij} & 0 \\ 0 & 0 & S_{ij} \end{bmatrix} \begin{Bmatrix} \varepsilon_j \\ \kappa_j \\ \gamma_m \end{Bmatrix}$$

$$\{F\} = [D]\{\varepsilon\}$$

where A_{ij}, B_{ij}, D_{ij} and S_{ij} are the extensional, bending–stretching coupling, bending and transverse shear stiffnesses. They may be defined as

$$A_{ij} = \sum_{k=1}^{n} \left(\overline{Q}_{ij}\right)_k (z_k - z_{k-1})$$

$$B_{ij} = \frac{1}{2} \sum_{k=1}^{n} \left(\overline{Q}_{ij}\right)_k (z_k^2 - z_{k-1}^2)$$

$$D_{ij} = \frac{1}{3} \sum_{k=1}^{n} \left(\overline{Q}_{ij}\right)_k (z_k^3 - z_{k-1}^3), \quad i,j = 1,2,6$$

$$S_{ij} = \kappa \sum_{k=1}^{n} \left(\overline{Q}_{ij}\right)_k (z_k - z_{k-1}), \quad i,j = 4,5$$

where κ is the transverse shear correction factor.

A.1. Element stiffness matrix

$$[k] = \int [B]^{\mathrm{T}} [D][B] \, \mathrm{d}x \, \mathrm{d}y$$

where $[B]$ is strain displacement matrix

$$[B] = \begin{bmatrix} \frac{\partial N_i}{\partial x} & 0 & \frac{N_1}{R_x} & 0 & 0 \\ 0 & \frac{\partial N_i}{\partial y} & \frac{N_1}{R_y} & 0 & 0 \\ \frac{\partial N_i}{\partial y} & \frac{\partial N_i}{\partial x} & 0 & 0 & 0 \\ 0 & 0 & 0 & \frac{\partial N_i}{\partial x} & 0 \\ 0 & 0 & 0 & 0 & \frac{\partial N_i}{\partial y} \\ C_0 \frac{\partial N_i}{\partial y} & C_0 \frac{\partial N_i}{\partial x} & 0 & \frac{\partial N_i}{\partial y} & \frac{\partial N_i}{\partial x} \\ -C_1 \frac{N_i}{R_x} & 0 & \frac{\partial N_i}{\partial x} & N_i & 0 \\ 0 & -C_1 \frac{N_i}{R_x} & \frac{\partial N_i}{\partial y} & 0 & N_i \end{bmatrix}, \quad i = 1, 2, \ldots, 8$$

A.2. Element mass matrix or consistent matrix

$$[m] = \int \int [N]^{\mathrm{T}} [P] [N] \, \mathrm{d}x \, \mathrm{d}y,$$

in which,

$$[N] = \begin{bmatrix} N_i & 0 & 0 & 0 & 0 \\ 0 & N_i & 0 & 0 & 0 \\ 0 & 0 & N_i & 0 & 0 \\ 0 & 0 & 0 & N_i & 0 \\ 0 & 0 & 0 & 0 & N_i \end{bmatrix}, \quad i = 1, 2, \ldots, 8$$

$$[P] = \begin{bmatrix} P_1 & 0 & 0 & P_2 & 0 \\ 0 & P_1 & 0 & 0 & P_2 \\ 0 & 0 & P_1 & 0 & 0 \\ P_2 & 0 & 0 & P_3 & 0 \\ 0 & P_2 & 0 & 0 & P_3 \end{bmatrix}$$

and

$$(P_1, P_2, P_3) = \sum_{k=1}^{n} \int_{z_{k-1}}^{z_k} (\rho)_k (1, z, z^2) \, \mathrm{d}z$$

A.3. Geometric stiffness matrix

$$[k_{\mathrm{G}}] = \int [G]^{\mathrm{T}} [S] [G] |J| \, \mathrm{d}v$$

in which,

$$[S] = \begin{bmatrix} s & 0 & 0 & 0 & 0 \\ 0 & s & 0 & 0 & 0 \\ 0 & 0 & s & 0 & 0 \\ 0 & 0 & 0 & s & 0 \\ 0 & 0 & 0 & 0 & s \end{bmatrix}$$

$$[s] = \begin{bmatrix} \sigma_x & \tau_{xy} \\ \tau_{xy} & \sigma_y \end{bmatrix}$$

$$[G] = \begin{bmatrix} \frac{\partial N_i}{\partial x} & 0 & 0 & 0 & 0 \\ \frac{\partial N_i}{\partial y} & 0 & 0 & 0 & 0 \\ 0 & \frac{\partial N_i}{\partial x} & 0 & 0 & 0 \\ 0 & \frac{\partial N_i}{\partial y} & 0 & 0 & 0 \\ \frac{-N_i}{R_x} & 0 & \frac{\partial N_i}{\partial x} & 0 & 0 \\ 0 & \frac{-N_i}{R_y} & \frac{\partial N_i}{\partial y} & 0 & 0 \\ 0 & 0 & 0 & \frac{\partial N_i}{\partial x} & 0 \\ 0 & 0 & 0 & \frac{\partial N_i}{\partial y} & 0 \\ 0 & 0 & 0 & 0 & \frac{\partial N_i}{\partial x} \\ 0 & 0 & 0 & 0 & \frac{\partial N_i}{\partial y} \end{bmatrix}, \quad i = 1, 2, 3, \ldots, 8$$

Finally, the overall structural matrices $[K]$, $[M]$ and $[K_G]$ can be obtained after assembling element matrices $[k]$, $[m]$ and $[k_G]$ respectively.

Appendix B

Let Q be the resultant shear force/unit width of plate at any cross section normal to x or y axis.

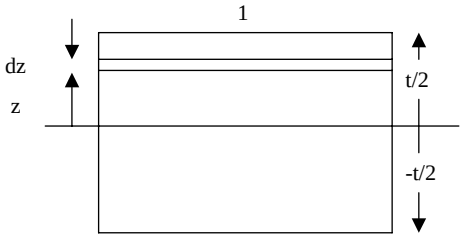

Case 1: Assuming the shear force induces an uniform shear stress and a constant shear strain over the depth, i.e. $\tau = Q/t$ as the width is unity.

The expression for strain energy of the plate per unit width is

$$U = \frac{1}{2}\int_0^L \int_A \frac{\tau^2}{G}\,\mathrm{d}a\,\mathrm{d}x = \frac{1}{2}\int_0^L \int_{-t/2}^{t/2} \frac{Q^2}{t^2 G}\,\mathrm{d}x\,\mathrm{d}z = \frac{1}{2}\int_0^L \frac{Q^2}{tG}\,\mathrm{d}x \tag{B.1}$$

Case 2: Considering the actual shear stress distribution over the depth (i.e. shear strain τ is not constant). The shear stress at any distance z from middle layer is

$$\tau = Q\frac{A\bar{z}}{I}. \tag{B.2}$$

Considering unit width of plate, the moment of the area $A\bar{z}$ can be expressed as

$$A\bar{z} = 1\left(\frac{t}{2} - z\right)\left[\frac{t}{2} - \left(\frac{t}{4} - \frac{z}{2}\right)\right] \tag{B.3}$$

or on simplification Eq. (B.3) reduces to

$$A\bar{z} = \frac{1}{8}(t^2 - 4z^2) \tag{B.4}$$

Substituting $I = t^3/12$ per unit width and Eq. (B.4) in Eq. (B.2), we get

$$\tau = \frac{Q}{I}A\bar{z} = Q\frac{1}{8}(t^2 - 4z^2)\frac{12}{t^3} \tag{B.5}$$

Substituting Eq. (B.5) in the expression for strain energy $U = \frac{1}{2}\int_0^L \int_A \frac{\tau^2}{G}\,\mathrm{d}a\,\mathrm{d}x$ and performing integration over the thickness we get

$$U = \frac{1}{2}\int_0^L \frac{Q^2}{(\frac{5}{6}G)t}\,\mathrm{d}x = \frac{1}{2}\int_0^L \frac{Q^2}{(\alpha G)t}\,\mathrm{d}x \quad \text{where } \alpha = 5/6 \tag{B.6}$$

Comparing Eqs. (B.1) and (B.6), it may be concluded that if one considers the average shear stress distribution and constant shear strain over the depth in the constitutive relationship, the effect of warping can be accounted by multiplying the rigidity modulus by a factor $\alpha = 5/6$, if the section is rectangular.

References

Adali, S., 1982. Stability of rectangular plates under nonconservative and conservative forces. International Journal of Solids and Structures 18 (12), 1043–1052.

Bazant, Z.P., 2000. Structural stability. International Journal of Solids and Structures 37, 55–67.

Bismarck-Nasr, M.N., 1992. Finite element analysis of aeroelasticity of plates and shells. ASME, Applied Mechanics Review 45 (12), 461–482.

Bismarck-Nasr, M.N., 1995. Dynamic stability of shallow shells subjected to follower forces. AIAA Journal 33 (2), 355–360.

Bolotin, V.V., 1963. Non-conservative Problems of the Theory of Elastic Stability. Pergamon Press, Oxford.

Chandrashekhara, K., 1989. Free vibrations of anisotropic laminated doubly curved shells. Computers and Structures 33 (2), 435–440.

Choo, Y.S., Kim, J.H., 2000. Dynamic stability of rectangular plates subjected to follower forces. AIAA Journal 38 (2), 353–361.

Cook, R.D., 1987. Concepts and Applications of Finite Element Analysis. John Wiley & Sons.

Culkowski, P.M., Reismann, H., 1977. Plate buckling due to follower edge forces. Transactions of ASME, Journal of Applied Mechanics 44, 768–769.

Datta, P.K., Deolasi, P.J., 1996. Dynamic instability characteristics of plates subjected to partially distributed follower edge loading with damping. Proc. Inst. Mech. Eng. (UK), Part C: Journal of Mechanical Engineering Science 210, 445–452.

Farshad, M., 1978. Stability of cantilever plates subjected to biaxial subtangential loading. Journal of Sound and Vibration 58 (4), 555–561.

Herrmann, G., 1967. Stability of equilibrium of elastic systems subjected to nonconservative forces. Applied Mechanics Review 20 (2), 103–108.

Herrmann, G., Jong, I.C., 1965. On the destabilizing effect of damping in nonconservative elastic systems. Journal of Applied Mechanics 32, 592–597.

Higuchi, K., Dowell, E.H., 1990. Dynamic stability of a rectangular plate with four free edges subjected to a follower force. AIAA Journal 28 (7), 1300–1306.

Higuchi, K., Dowell, E.H., 1992. Effect of structural damping on flutter of plates with follower force. AIAA Journal 30 (3), 820–825.

Kim, J.H., Kim, H.S., 2000. A study on the dynamic stability of plate under follower force. Computers and Structures 74, 351–363.

Kim, J.H., Park, J.H., 1998. On the dynamic stability of rectangular plates subjected to intermediate follower forces. Journal of Sound and Vibration, Letters to the Editor 209 (5), 882–888.

Komarakul-Na-Nakoran, A., Arora, J.S., 1990. Stability criteria: a review. Computers and Structures 37 (1), 35–49.

Langthjem, M.A., Sugiyama, Y., 2000. Dynamic stability of columns subjected to follower loads: a survey. Journal of Sound and Vibration 238 (5), 809–851.

Leipholz, H.H.E., 1978. Stability of rectangular simply supported plate subjected to nonincreasing tangential follower forces. Journal of Applied Mechanics 45, 223–224.

Leipholz, H.H.E., Pfendt, F., 1983. Application of extended equations of Galerkin to stability problems of rectangular plates with free edges subjected to uniformly distributed follower forces. Computer Methods in Applied Mechanics and Engineering 37, 341–365.

Librescu, L., Khdeir, A.A., Fredcrik, D., 1989. A shear deformable theory of laminated composite shallow shell-type panels and their response analysis I: free vibration and buckling:. ACTA Mechanica 76, 1–33.

Liew, K.M., Lim, C.W., Kitipornchai, S., 1997. Vibration of shallow shells: a review with bibliography. Applied Mechanics Review, ASME 50 (8), 431–444.

Park, S.H., Kim, J.H., 2000a. Dynamic stability of a completely free circular cylindrical shell subjected to a follower force. Journal of Sound and Vibration 231 (4), 989–1005.

Park, S.H., Kim, J.H., 2000b. Dynamic stability of a free–free cylindrical shell under follower force. AIAA Journal 38 (6), 1070–1077.

Park, S.H., Kim, J.H., 2002. Dynamic stability of a stiff-edged cylindrical shell subjected to a follower force. Computers and Structures 80 (3–4), 227–233.

Qatu, M.S., 1992. Review of shallow shell vibration research. Shock and Vibration Digest 24 (9), 285–300.

Qatu, M.S., Leissa, A.W., 1991. Natural frequencies for cantilevered doubly curved laminated composite shallow shells. Composite Structures 17, 227–255.

Reddy, J.N., 1984. Exact solutions of moderately thick laminated shells. Journal of Engineering Mechanics ASCE 110, 794–809.

Ryu, B.J., Sugiyama, Y., 1994. Dynamic stability of cantilevered Timoshenko columns subjected to rocket thrust. Computers and Structures 51, 331–335.

Sahu, S.K., Datta, P.K., 2001. Parametric instability of doubly curved panels subjected to nonuniform harmonic loading. Journal of Sound and Vibration 240 (1), 117–129.

Sciuva, M.D., Carrera, E., 1990. Static buckling of moderately thick, anisotropic, laminated and sandwich cylindrical shell panels. AIAA Journal 28, 1782–1793.

Wu, J.J., 1976. On missile stability. Journal of Sound and Vibration 49 (1), 141–147.